Concept Paper

It from Qubit: How to Draw Quantum Contextuality[†]

Michel Planat

Institut FEMTO-ST, Centre National de la Recherche Scientifique, 32 Avenue de l'Observatoire, 25044 Besançon, France; E-Mail: michel.planat@femto-st.fr

Abstract: Wheeler's observer-participancy and the related it from bit credo refer to quantum non-locality and contextuality. The mystery of these concepts slightly starts unveiling if one encodes the (in)compatibilities between qubit observables in the relevant finite geometries. The main objective of this treatise is to outline another conceptual step forward by employing Grothendieck's *dessins d'enfants* to reveal the topological and (non)algebraic machinery underlying the measurement acts and their information content.

Keywords: it from bit; quantum contextuality; graphs; *dessin d'enfant*; projective plane

1. Introduction

I can no better summarize the topic of this essay than by borrowing the opinions of three giants of physics, namely of John Wheeler on " it from bit", of John Bell on " nonlocality" and of David Mermin on " contextuality" (I could also have referred to Asher Peres).

Wheeler [1]: *We have clues, clues most of all in the writings of Bohr, but not answer ... Are billions upon billions of acts of observer-participancy the foundation of everything? We are about as fast as we can today from knowing enough about the deeper machinery of the universe to answer this question. Increasing knowledge about detail has brought an increasing ignorance about the plan.*

Wheeler [2]: *It from bit. Otherwise put, every it—every particle, every field of force, even the space time continuum itself—derives its function, its meaning, its very existence entirely—even if in some contexts indirectly—from the apparatus-elicited answers to yes or no questions, binary choices, bits.*

Bell [3]: *In a theory in which parameters are added to quantum mechanics to determine the results of individual measurements, without changing the statistical predictions, there must be a mechanism whereby the setting of one measuring device can influence the reading of another instrument, however remote. Moreover, the signal involved must propagate instantaneously, so that a theory could not be Lorentz invariant.*

Mermin [4]: *It is also appealing to see the failure of the EPR reality criterion emerge quite directly from the one crucial difference between the elements of reality (which, being ordinary numbers, necessarily commute) and the precisely corresponding quantum mechanical observables (which sometimes anticommute).*

On the mathematical side, my arguments will rely on another eminent figure of science, *viz.*:

Grothendieck [5]: *In the form in which Belyi states it, his result essentially says that every algebraic curve defined over a number field can be obtained as a covering of the projective line ramified only over the points* 0, 1 *and* ∞. *The result seems to have remained more or less unobserved. Yet it appears to me to have considerable importance. To me, its essential message is that there is a profound identity between the combinatorics of finite maps on the one hand, and the geometry of algebraic curves defined over number fields on the other. This deep result, together with the algebraic interpretation of maps, opens the door into a new, unexplored world - within reach of all, who pass by without seeing it.*

Why do I refer to Grothendieck? My first point is that Wheeler's observer-participancy is contextual: the *it* does not preexist to the measurement set-up, and (the it from bit extraction being even more intriguing) the measured value depends on all mutually compatible measurements. Second, a compatibility (*i.e.*, commutativity) diagram of observables itself has a kind of engine that drives it. The hidden engine is, in my opinion, nothing but Grothendieck's *dessin d'enfant* (a child's drawing) [6]. The relevant "quantum" graphs that we will encounter on our journey are mainly commuting/anticommuting graphs discovered by Mermin. We will ask ourselves the question whether, and how, a *dessin d'enfant* (an algebraic curve in the sense of Grothendieck) can be associated with the contextual set-up behind such a graph. Interestingly enough, also confirming the it from bit claim, a relevant "contextual' graph may have more Shannon capacity/information than expected in a perfect graph. This sounds in resonance with Shor's quantum algorithm, which allows factoring of integers in polynomial time instead of the exponential one (more information in less time).

It will suffice to play with the so-called Pauli groups of operators/observables for two or three parties, *i.e.*, two- or three-qubit systems: Alice, Bob and/or Charlie set-ups. Most importantly, experiments with compatible (mutually commuting) operators make sense; otherwise, the results are expected to be fully independent [7]. Some years ago, it was realized that to mathematically grasp the essence of these (in)compatibilities, finite geometries have to be called on [8]. In what follows, it will be demonstrated that to get further insights in this respect, the concept of a *dessin d'enfant*—a bipartite graph embedded on an oriented surface—must enter the game. Any *dessin* can be given the structure of a Riemann surface, and the Riemann surfaces arising this way are those defined over the field of algebraic numbers (Belyi's theorem). This subject is briefly described in Section 2.

If one considers the fifteen two-qubit operators (the identity matrix is discarded), here, the underlying geometry—the smallest non-trivial generalized quadrangle—tells us a lot about the higgledy-piggledy collection of potential two-qubit experiments [8]. However, as emphasized by Mermin [7], to unify all relevant concepts pertinent to non-locality and contextuality, one needs three parties. Here, a fundamental building block is a heptad of mutually commuting operators forming the smallest projective plane, the Fano plane, having seven points and dually seven lines, with three points per line and three lines through a point. In Section 2.1, the seven points of the Fano plane are put in a bijective correspondence with the edges of a tree-like *dessin d'enfant*, ensuring its algebraicity (in Grothendieck's sense). The symmetry group permuting the edges of the *dessin* and stabilizing the lines of the Fano plane is the well-known simple group of cardinality 168.

Then, in Section 3.1, I invoke a square graph with eight vertices, with mutually commuting or anticommuting operators, for a proof of Bell's theorem about non-locality. Here, the graph is itself the *dessin* and is thus algebraic. Section 3.2 starts a non-trivial story about contextuality and the so-called Kochen-Specker theorem as told by Mermin. We only need a two-player (two-qubit) set-up. The graph is a "magic" square (a three-by-three grid) embodying a contradiction between the algebra of operators and eigenvalues [7]. We shall uncover in its shadow an interesting algebraic curve/*dessin d'enfant*, displayed here for the first time. The symmetry group permuting the nine edges of the *dessin* and stabilizing the lines of the magic square has order 72. Finally, in Section 3.3, as expected, both a contextual and "magic" array of three-qubit observables comes, the so-called Mermin's pentagram. This graph occurs in another disguise: the Petersen graph, being thus embeddable as a polyhedron in the real projective plane. Such a pentagram is one of a totality of $12,096$ guys fitting the structure of the smallest exceptional Lie geometry—the split Cayley hexagon of order two [9,10].

2. What Is a Dessin D'enfant?

... here I was brought back, via objects so simple that a child learns them while playing, to the beginnings and origins of algebraic geometry, familiar to Riemann and his followers! [5].

Details can be found in [5,11–13]. See also [14] for a link to Feynman diagrams.

Step 1 (easy): A *dessin d'enfant* (child's drawing) is a map drawn on a surface (a smooth compact orientable variety of dimension two) such that vertices are points, edges are arcs connecting the vertices and the complement of the graph is the union of faces (each one homeomorphic to the open disk of $\mathbb{R}^2$). The graph may feature multiple edges and/or loops, but has to be connected. Taking S, A and F for the number of vertices, edges and faces, respectively, the genus, g, of the map is given by Euler's formula $S - A + F = 2 - 2g$.

Step 2 (still easy): Convert the graph of Step 1 into a bipartite graph by regarding its vertices as black and placing a white vertex in each of its edges. The set of half-edges so defined is encoded by a permutation group $P = \langle \alpha, \beta \rangle$; here, the permutation, α, respectively β) rotates the half-edges around each black (resp. white) vertex in accord with the cyclic ordering in that vertex. The cycle structure for the faces follows from the permutation γ satisfying $\alpha\beta\gamma = 1$. The Euler characteristic now reads $2 - 2g = B + W + F - n$, where B, W and n stands, respectively, for the number of black vertices, the number of white vertices and the number of half-edges.

It is also known that maps on connected oriented surfaces are parametrized by the conjugacy classes of the subgroups of the triangle group, also called the cartographic group by Grothendieck,

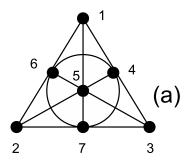$$C_2^+ = \langle \rho_0, \rho_1, \rho_2 | \rho_1^2 = \rho_0\rho_1\rho_2 = 1 \rangle \tag{1}$$

The possible existence of a *dessin d'enfant* of prescribed properties (permutation group, cycle structure) can thus be checked from a systematic enumeration of conjugacy classes of C_2^+.
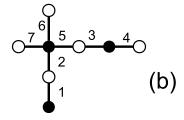
Step 3 (difficult): The Belyi theorem states that to a combinatorial map (defined in Step 2), there corresponds a Riemann surface, X, defined over the field, $\bar{\mathbb{Q}}$, of algebraic numbers. This happens if, and only if, there exists a covering $f : X \to \bar{\mathbb{C}}$ unramified outside $\{0, 1, \infty\}$. The covering (an algebraic curve), f, associated with a *dessin d'enfant* is, in general, very difficult to find explicitly, except for simple cases devoid of loops. Klein, as early as 1884, was the first to get them for the graphs representing Platonic solids [15].

2.1. The Fano Plane and Its Curve

A finite projective plane is a point-line incidence geometry, such that: (i) any two lines meet in a unique point; (ii) any two distinct points are on a unique line; and (iii) there are at least four points, not three of them collinear. The simplest case is the projective plane of order two—the Fano plane. Projective planes are conjectured to exist only if their order is a power of a prime number.

Figure 1. (**a**) The Fano plane, $\mathcal{F}$, and (**b**) a corresponding *dessin d'enfant*, $\mathcal{D}_\mathcal{F}$. The permutation group characterizing $\mathcal{D}_\mathcal{F}$ is $P = \langle \alpha, \beta \rangle$, with $\alpha = (1)(2, 7, 6, 5)(3, 4)$ and $\beta = (1, 2)(3, 5)(4)(6)(7)$. One has $B = 3$ black vertices, $W = 5$ white vertices, $n = 7$ half-edges, $F = 1$ face and genus $g = 0$.

As already mentioned, a three-qubit maximal commuting set may be seen as a heptad of points/lines satisfying the axioms of a Fano plane [16]. The seven points are mapped to the seven three-qubit operators, and each line features a triple of mutually commuting operators whose product is $\pm$, the identity matrix. We are in the search of a *dessin d'enfant*, $\mathcal{D}_\mathcal{F}$, whose edges can be put in a bijective

correspondence with the points of the Fano plane, $\mathcal{F}$, in such a way that the permutation group, P, of $\mathcal{D}_{\mathcal{F}}$ acts transitively on the lines of $\mathcal{F}$ and stabilize them. One knows that $P = PSL(2,7)$, the simple group of order 168. Using the software, Magma, we are able to compute the 131 subgroups of index seven of the cartographic group, C_2^+, extract the 10 of them whose group of cosets is isomorphic to P and also have the right action on $\mathcal{F}$. One choice is depicted in Figure 1, as reproduced from [11] (p. 17 and p. 50); the corresponding Belyi map is the polynomial:

$$Z = \sqrt{8}z^4(z-1)^2(z-a) \text{ with } a = (-1 - i\sqrt{7})/4 \tag{2}$$

3. Dessins D'enfants, Non-Locality and Contextuality

3.1. A Dessin D'enfant for Bell's Theorem

Let us recall now that for dichotomic observables $\sigma_i^2 = \pm 1$, $i = 1, 2, 3, 4$, when giving the pair (σ_1, σ_3) to Bob and the pair (σ_2, σ_4) to Alice, the Bell-CHSH (Clauser-Horne-Shimony-Holt) approach consists of defining the number

$$C = \sigma_2(\sigma_1 + \sigma_3) + \sigma_4(\sigma_3 - \sigma_1) = \pm 2 \tag{3}$$

and observing the Bell-CHSH inequality [17] (p. 164)

$$|\langle \sigma_1 \sigma_2 \rangle + \langle \sigma_2 \sigma_3 \rangle + \langle \sigma_3 \sigma_4 \rangle - \langle \sigma_4 \sigma_1 \rangle| \leq 2 \tag{4}$$

where $\langle \rangle$ here means that we are taking averages over many experiments. Bell's theorem simply means finding a violation of the aforementioned inequality with quantum observables and dichotomic eigenvalues. A simple choice is the quadruple:

$$(\sigma_1 = IX, \ \sigma_2 = XI, \ \sigma_3 = IZ, \ \sigma_4 = ZI) \tag{5}$$

where X, Y and Z are the ordinary Pauli spin matrices, and one uses the short-hand notation for the tensor product, e.g., $IX \equiv I \otimes X$. Thus, $\sigma_i^2 = 1$, and one finds that

$$C^2 = 4*I + [\sigma_1, \sigma_3][\sigma_2, \sigma_4] = 4 \begin{pmatrix} 1 & . & . & 1 \\ . & 1 & \bar{1} & . \\ . & \bar{1} & 1 & . \\ 1 & . & . & 1 \end{pmatrix} \tag{6}$$
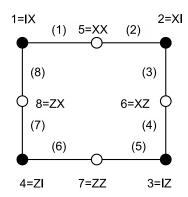
has eigenvalues zero and eight, both of multiplicity two. Taking the norm of the bounded linear operator, A, as $||A|| = sup(||A\psi||/||\psi||)$, $\psi \in \mathcal{H}$ (the relevant Hilbert space), one gets the maximal violation of the Bell-CHSH inequality [17] (p. 174):

$$||C|| = 2\sqrt{2} \tag{7}$$

A straightforward computer check shows that there are 90 such distinct proofs of Bell's theorem with two-qubit operators and as many as $30,240$ ones with three-qubit ones, all of them yielding a maximal violation of the Bell-CHSH inequality. These numbers are intimately connected with the structure of the corresponding contextual spaces.
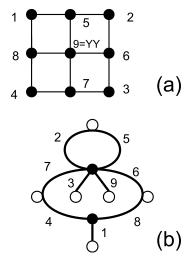
Figure 2. The commutation/anti-commutation diagram for Bell's theorem is, at the same time, a *dessin d'enfant* with permutation group $P = \langle \alpha, \beta \rangle = D_4$, where $\alpha = (1,8)(2,3)(4,5)(6,7)$, $\beta = (1,2)(3,4)(5,6)(7,8)$ and the bracketed half-edge labeling.

Let us represent the commutation relations between the elements of Equation (5) as illustrated in Figure 2, where the black vertices are labeled by $i \equiv \sigma_i$, and a white vertex represents the operator that is the product of the two operators at the endpoints of the corresponding edge (e.g., $5 = \sigma_1\sigma_2 = IX.XI = XX$); it is worth noting that three operators placed along the same straight-line segment mutually commute, as do two "white" operators situated opposite each other. This is a remarkable instance where the commutation/anti-commutation diagram is bipartite and, as it stands, it also represents a *dessin d'enfant* (with the permutation group equal to the dihedral group, D_4, on eight elements). The algebraic curve (Belyi map) associated with it is well known (it was already derived by Klein [15] (p. 106)):

$$Z = \frac{(z^4 - 1)^2}{-4z^4} \tag{8}$$

Figure 3. (**a**) The Mermin square, $\mathcal{M}$, and (**b**) its associated *dessin d'enfant*, $\mathcal{D}_\mathcal{M}$, with permutation group $P = \langle \alpha, \beta \rangle$, where $\alpha = (3,9,6,5,2,7)(1,8,4))$, $\beta = (1)(3)(9)(2,5)(4,7)(6,8)$. One has $B = 2$ black vertices, $W = 6$ white vertices, $N = 9$ half-edges, $F = 3$ faces and genus $g = 0$.

3.2. Mermin's Square

Let us now have a bit more of a careful look at Figure 2. We observe that the product of the two observables associated with a pair of the opposite white vertices is the same, YY. By supplying this "missing" vertex and the two lines passing through it, we get a 3×3 grid (as illustrated in Figure 3a). This grid is a remarkable one: all triples of observables located in a row or a column have their product equal to $+II$ except for the middle column, where $XX.YY.ZZ = -II$. Mermin was the first to observe that this is a Kochen-Specker (parity) -type contradiction, since the product of all triples yields the matrix, $-II$, while the product of corresponding eigenvalues is $+1$ (since each of the latter occurs twice, once in a row and once in a column) [7]. Such a Mermin "magic" square may be used to provide many contextuality proofs from the vectors shared by the maximal bases corresponding to a row/column of the diagram. The simplest, so-called $(18, 9)$ one (18 vectors and nine bases) has, remarkably, the orthogonality diagram, which is itself a Mermin square (nine vertices for the bases and 18 edges for the vectors) [10] (Equation (6)).

Now, we would like to represent our Mermin square, $\mathcal{M}$, in a way analogous to what we did for the Fano plane in Section 2.1, that is we would like to draw a *dessin d'enfant*, $\mathcal{D}_{\mathcal{M}}$, whose nine half-edges are in a bijective correspondence with the vertices of $\mathcal{M}$ and whose permutation group, P, acts transitively on the rows/columns of $\mathcal{M}$ by stabilizing them. The symmetry group of $\mathcal{M}$ is isomorphic to $\mathbb{Z}_3^2 \rtimes \mathbb{Z}_2^3$, a group of order 72. Using again the software, Magma, we searched for all $1,551$ subgroups of index nine in the cartographic group, C_2^+, defined in Equation (1), extracted the two subgroups isomorphic to P and selected the one having the right action on $\mathcal{M}$; the corresponding *dessin d'enfant*, $\mathcal{D}_{\mathcal{M}}$, is shown in Figure 3b.

Actually, the dessin in Figure 3b stabilizes the Hesse configuration that consists of the union of two (3×3)-grids: the one $\mathcal{M}$ shown in Figure 3a and the one obtained from the maximal sets of mutually non-collinear pairs of points of $\mathcal{M}$. A single (3×3)-grid can be stabilized from a genus one dessin; see [6] (Figure 7).

3.3. Mermin's Pentagram

Poincaré [18] (p. 342); *Perceptual space is only an image of geometric space, an image altered in shape by a sort of perspective.*

Weyl [18] (p. 343): *In this sense the projective plane and the color continuum are isomorphic with one another.*
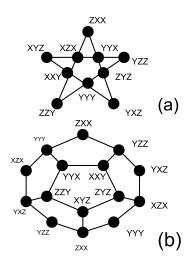
Color experience through our eyes to our mind relies on the real projective plane, $\mathbb{RP}^2$ [18]. Three-qubit contextuality also relies on $\mathbb{RP}^2$ thanks to a Mermin "magic" pentagram, which, for reasons explained below in (i), we denote $\bar{\mathcal{P}}$ (by abuse of language, because we are at first more interested to see the pentagram as a geometrical configuration than as a graph). One such pentagram is displayed in Figure 4a. It consists of a set of five lines, each hosting four mutually commuting operators and any two sharing a single operator. The product of operators on each of the lines is $-III$, where I is the 2×2 identity matrix. It is impossible to assign the dichotomic truth values ± 1 to eigenvalues, while keeping the multiplicative properties of operators, so that the Mermin pentagram is, like its two-qubit sibling, "magic" and, so, contextual [4,8–10].

Let us enumerate a few remarkable facts about a pentagram.

(i) The graph, $\bar{\mathcal{P}}$, of a pentagram is the complement of that of the celebrated Petersen graph, $\mathcal{P}$. One noticeable property of $\mathcal{P}$ is to be the smallest bridgeless cubic graph with no three-edge-coloring. The Petersen graph is thus not planar, but it can be embedded without crossings on $\mathbb{RP}^2$ (one of the simplest non-orientable surfaces), as illustrated in Figure 4b.

(ii) There exist altogether $12,096$ three-qubit Mermin pentagrams, this number being identical to that of the automorphisms of the smallest split Cayley hexagon, $G_2(2)$—a remarkable configuration of 63 points and 63 lines, whose structure is fully encoded in that of the Fano plane [8].

Figure 4. (**a**) A Mermin pentagram, $\bar{\mathcal{P}}$, and (**b**) the embedding of the associated Petersen graph, $\mathcal{P}$, on the real projective plane as a hemi-dodecahedron.

(iii) Now comes an item close to the it from bit perspective, if one employs the so-called Shannon capacity of $\bar{\mathcal{P}}$. The Shannon capacity, $\Theta(G)$, of a graph, G, is the maximum number of k-letter messages than can be sent through a channel without the risk of confusion. One knows that $\Theta(G)$ has for its lower bound the size, $\alpha(G)$, of a maximum independent set and for its upper bound the Lovász number, $\theta(G)$ [19]. For the complement graph, $\bar{G}$, the Lovász number, $\theta(\bar{G})$, is found to lie between the clique number, $\omega(G)$, and the chromatic number, $\kappa(G)$. For the Petersen graph, this leads to $2 \leq \Theta(P) \leq 4$ (one knows from [19] that $\Theta(P) = 4$) and for the pentagram graph, $2 \leq \theta(\bar{P}) \leq 3$. A direct calculation yields $\Theta(\bar{P}) \geq \sqrt{5}$ [9,10]. Note hat the pentagon graph attains the tight bound, $\sqrt{5}$, and that one also found $\Theta(\bar{P}) = 5/2$ for the Petersen graph [20]. See also [21] for a review and [22] for another viewpoint.

(iv) Does there exist a *dessin d'enfant* for the pentagram? In view of the relationship of $\bar{P}$ to the non-orientable $\mathbb{RP}^2$, this was first found rather unlikely. A genus zero dessin allowing the stabilization of Mermin's pentagram was finally discovered in [6] (Figure 10). It is shown in [6] (Section 4.5) how Mermin's pentagram, the Petersen graph, Desargues configuration and the hemi-dodecahedron are just different projections of the same object, giving credit to the Lewis Caroll parabola.

Let us conclude this essay by an excerpt from Lewis Carroll's tale: " The hunting of the snark"

"What's the good of Mercator's North Poles and Equators,

Tropics, Zones, and Meridian Lines?"

So the Bellman would cry: and the crew would reply

"They are merely conventional signs!"

Acknowledgments

Conflicts of Interest

The author declares no conflict of interest.

References

1. Wheeler, J.A. Law without law. In *Quantum Theory and Measurement*; Wheeler, J.A., Zurek, W.H., Eds.; Princeton University Press: Princeton, MA, USA, 1983.
2. Wheeler, J.A. Information, physics, quantum: The search for links. In *Complexity, Entropy, and the Physics of Information*; Zurek, W., Ed.; Addison-Wesley: Redwood, CA, USA, 1990.
3. Bell, J.S. On the Einstein-Podolsky-Rosen paradox. *Physics* **1964**, *1*, 195–200.
4. Mermin, N.D. What's wrong with these elements of reality. *Phys. Today* **1990**, *43*, 9–11.
5. Grothendieck, A. Sketch of a programme. In *Geometric Galois Actions 1. Around Grothendieck's Esquisse d'un Programme*; Schneps, L., Lochak, P., Eds.; Cambridge University Press: Cambridge, UK, 1997; pp. 243–283.
6. Planat, M.; Giorgetti, A.; Holweck, F.; Saniga, M. Quantum contextual finite geometries from *dessins d'enfants*. **2013**, arXiv:1310.4267v2 [quant-ph].
7. Mermin, N.D. Hidden variables and two theorems of John Bell. *Rev. Mod. Phys.* **1993**, *65*, doi: http://dx.doi.org/10.1103/RevModPhys.65.803.
8. Saniga, M.; Planat, M. Multiple qubits as symplectic polar spaces of order two. *Adv. Studies Theor. Phys.* **2007**, *1*, 1–4.
9. Planat, M.; Saniga, M.; Holweck, F. Distinguished three-qubit 'magicity' via automorphisms of the split Cayley hexagon. *Quant. Inf. Process.* **2013**, *12*, 2535–2549.
10. Planat, M. On small proofs of the Bell-Kochen-Specker theorem for two, three and four qubits. *Eur. Phys. J. Plus* **2012**, *127*, 1–11.
11. Schneps, L., Lochak, P., Eds. *Geometric Galois Actions 2. The inverse Galois problem, Moduli Spaces and Mapping Class Groups*; Cambridge University Press: Cambridge, UK, 1997.
12. Schneps, L., Ed. *The Grothendieck Theory of Dessins d'Enfants*; Cambridge University Press: Cambridge, UK, 1994.
13. Lando, S.K.; Zvonkin, A.K. *Graphs on Surfaces and Their Applications*; Springer: Berlin, Germany, 2004.
14. Koch, R.M.; Ramgoolam, S. From matrix models and quantum fields to Hurwitz space and the absolute Galois group. **2010**, arXiv:1002.1634v1 [hep-th].
15. Klein, F. *The Icosahedron and the Solutions of Equations of the Fifth Degree*; Dover: New York, NY, USA, 1956.

16. Lévay, P.; Saniga, M.; Vrana, P. Three-qubit operators, the split Cayley hexagon of order two and black holes. *Phys. Rev. D* **2008**, *78*, 124022.

17. Peres, A. *Quantum theory: Concepts and Methods*; Kluwer: Dordrecht, The Netherlands, 1995.

18. Flanagan, B.J. Are perceptual fields quantum fields? *NeuroQuantology* **2003**, *1*, 334–364.

19. Lovász, L. On the Shannon capacity of a graph. *IEEE Trans. Inf. Theory* **1979**, *25*, 1–7.

20. Cabello, A.; Severini, S.; Winter, A. (Non-)Contextuality of physical theories as an axiom. **2010**, arXiv:1010.2163 [quant-ph].

21. Acín, A.; Fritz, T.; Leverrier, A.; Sainz, A.B. A combinatorial approach to nonlocality and contextuality. **2012**, arXiv:1212.4084 [quant-ph].

22. Arkhipov, A. Extending and characterizing quantum magic games. **2012**, arXiv:1209.3819 [quant-ph].